Synthesis of cubic $SrCoO_3$ single crystal and its anisotropic magnetic and transport properties

J. Phys.: Condens. Matter **23** (2011) 245601 (6pp) doi:10.1088/0953-8984/23/24/245601

Synthesis of cubic $SrCoO_3$ single crystal and its anisotropic magnetic and transport properties

Youwen Long[1,4], Yoshio Kaneko[1], Shintaro Ishiwata[2,3], Yasujiro Taguchi[2] and Yoshinori Tokura[1,2,3]

[1] Multiferroics Project, Exploratory Research for Advanced Technology, Japan Science and Technology Agency, c/o RIKEN Advanced Science Institute, Wako 351-0198, Japan
[2] Cross-Correlated Materials Research Group (CMRG) and Correlated Electron Research Group (CERG), RIKEN Advanced Science Institute, Wako 351-0198, Japan
[3] Department of Applied Physics and Quantum-Phase Electronics Center (QPEC), University of Tokyo, Hongo, Tokyo 113-8656, Japan

E-mail: ywlong@riken.jp

Received 11 February 2011, in final form 13 May 2011
Published 1 June 2011
Online at stacks.iop.org/JPhysCM/23/245601

Abstract
A large-size single crystal of nearly stoichiometric $SrCoO_3$ was prepared with a two-step method combining the floating-zone technique and subsequent high oxygen pressure treatment. $SrCoO_3$ crystallizes in a cubic perovskite structure with space group $Pm\bar{3}m$, and displays an itinerant ferromagnetic behavior with the Curie temperature of 305 K. The easy magnetization axis is found to be along the [111] direction, and the saturation moment is 2.5 μ_B/f.u., in accord with the picture of the intermediate spin state. The resistivity at low temperatures (T) is proportional to T^2, indicative of the possible effect of orbital fluctuation in the intermediate spin ferromagnetic metallic state. Unusual anisotropic magnetoresistance is also observed and its possible origin is discussed.

(Some figures in this article are in colour only in the electronic version)

1. Introduction

Cobalt oxides have attracted great attention due to their interesting structural and physical properties as well as potential applications as solid-state fuel cells [1, 2]. For a $Co^{3+}(3d^6)$ ion in an octahedral crystal field, its electronic configuration or spin state sensitively depends on external physical parameters such as temperature and pressure, reflecting the subtle energy balance among the crystal field splitting ($10Dq$), the Hund's-rule coupling, and the electron transfer energy. In $LaCoO_3$, for example, the spin state of the Co^{3+} ion changes from low spin ($S = 0$) to intermediate spin ($S = 1$) or high spin ($S = 2$) as the temperature is increased [3–6]. In contrast to the low spin ground state of $LaCoO_3$, a high spin $S = 2$ state emerges in the ground state of $BiCoO_3$ [7]. However, this high spin state is not so robust and is easily transformed to the intermediate or low spin state by application of high pressure around 3 GPa [8].

The valence states of Co ions are quite variably dependent on chemical compositions and synthesis conditions as well. An interesting example is provided by the $SrCoO_{3-\delta}$ ($0 \leqslant \delta \leqslant 0.5$) system, where the oxygen nonstoichiometry governs the structural and physical properties. As is well known, $SrCoO_{2.5}$ ($\delta = 0.5$) crystallizes in an orthorhombic brownmillerite-type structure [9, 10]. Like for $BiCoO_3$, a high spin state with $S = 2$ is present in this material. With the oxygen deficiency decreasing to $\delta \approx 0.25$, the structure becomes cubic [11]. As δ is further reduced to about 0.15, tetragonal distortion is found to emerge [12]. In the end for compound $SrCoO_3$, the cubic symmetry with space group $Pm\bar{3}m$ appears again [13]. Because the 3d energy level of Co^{4+} ion is quite deep, partial charge transfer from ligand to metal (i.e., p–d hybridization) is present in $SrCoO_3$ [14]. Like for other transition metal oxides with unusually high valence states, such

[4] Author to whom any correspondence should be addressed.

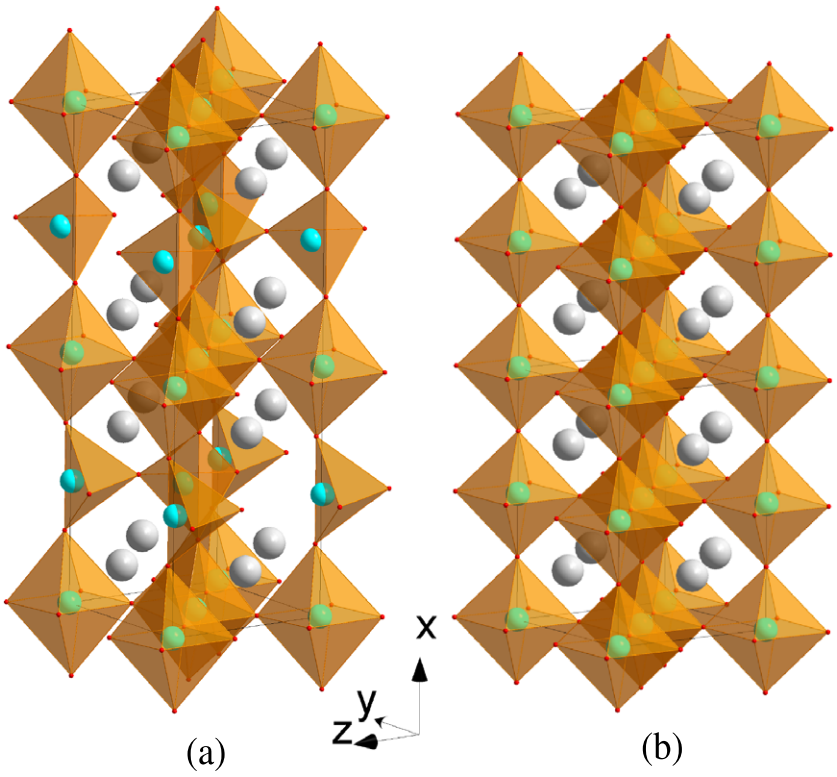

Figure 1. Crystal structure of (a) orthorhombic brownmillerite-type $SrCoO_{2.5}$, and (b) cubic perovskite-type $SrCoO_3$. To show the similarity of these structures, a $4 \times \sqrt{2} \times \sqrt{2}$ supercell is shown in (b). The large gray and small red spheres stand for Sr and O atoms, respectively, and medium-sized green and cyan spheres correspond to Co atoms with sixfold and fourfold coordination.

as Fe^{4+}, Ni^{3+}, and Cu^{3+}, negative charge transfer energy Δ appears in $SrCoO_3$. A unique characteristic of $SrCoO_3$ among these materials with negative Δ is that this compound exhibits ferromagnetic (FM) ordering with a high Curie temperature (T_c) [13, 15, 16]. Although there have been many studies on $SrCoO_3$, chemically stoichiometric single crystal has not been obtained as yet. As a result, physical properties such as the FM Curie temperature and the resistivity are sample dependent due to the different oxygen deficiencies and/or grain boundary effects in polycrystalline samples. In particular, the spin state of Co^{4+} in $SrCoO_3$ has been a subject of active debate. Most experimental results have shown that the Co^{4+} is basically in a low spin state [17–21]. However, theoretical calculations have predicted that the low spin state cannot be a stable ground state, and that the most probable spin configuration should be an intermediate spin state [14, 22]. To gain more insight into the intrinsic physical properties, it is necessary to obtain a sizable single crystal with as little oxygen deficiency as possible.

There have been reported some attempts to synthesize a $SrCoO_3$ single crystal by a floating-zone method. However, greatly oxygen-deficient single crystals, such as $SrCoO_{2.64}$ and $SrCoO_{2.70}$, were only obtained due to the limitation of oxygen pressure [23, 24]. As shown in figure 1, the structure of brownmillerite-type $SrCoO_{2.5}$ is composed of alternating CoO_6 octahedron and CoO_4 tetrahedron layers along the x-axis. This can be viewed as a modified perovskite structure with the ordered oxygen deficiency along the [011] direction with a cubic setting, as described in [9]. If additional oxygen atoms can fully occupy the deficient positions with the aid of high pressure, then a perovskite structure may be obtained from the brownmillerite one. Therefore, an opportunity to obtain $SrCoO_3$ single crystal is provided by treating the oxygen-deficient brownmillerite-type $SrCoO_{2.5}$ single crystal under extremely high oxygen pressure.

In this paper, we report the successful synthesis of large-size, nearly stoichiometric $SrCoO_3$ single crystal and its anisotropic magnetic and transport properties. The T_c ($\sim$305 K) observed for our crystal is higher than any other reported result for polycrystalline samples, by at least 20 K. The saturation moment obtained indicates that the spin configuration of the Co^{4+} ion is close to an intermediate spin state. Although this compound possesses a highly symmetric cubic structure, it shows significant anisotropic magnetoresistance (AMR) with fields applied along different crystal axes.

2. Experimental details

As the first step of the crystal synthesis, a brownmillerite-type $SrCoO_{2.5}$ polycrystalline sample was prepared by solid-state reaction using analytical purity $SrCO_3$ and Co_3O_4 with a 3:1 molar ratio as starting materials. After completely mixing the reagents, they were heated at 1173 K for 12 h. Then the product was ground again and pressed into a rod 5 mm in diameter and 10 cm in length. A second heat treatment was carried out for the rod at 1373 K for 12 h, followed by a quick quenching into

liquid N_2 [10, 25]. Thus, the polycrystalline brownmillerite phase was obtained. The brownmillerite-type single crystal was grown by using a lamp-image-type floating-zone furnace in flowing Ar gas. The isostructural $SrFeO_{2.5}$ single crystal was used as a seed. The growth rate was 2 mm h^{-1}, and the rotation speeds for the grown crystal and the feeding rod were 20 rpm in opposite directions. Finally, the oxygen-deficient $SrCoO_{2.5}$ single crystal was treated in a cubic-anvil-type high pressure apparatus at 6.5 GPa and 1023 K for 1 h with the presence of $KClO_4$ oxidizing agent, which was put all around the $SrCoO_{2.5}$ crystal. The typical size of sample for the high pressure treatment was 2 mm in diameter and 4 mm in length.

Powder x-ray diffraction (XRD) was used to investigate pulverized crystals, using a Rigaku diffractometer with Cu Kα radiation (40 kV, 300 mA). The back-reflection Laue method was applied to confirm that the sample was indeed a single crystal and also to determine the orientation of the crystal axes. A thermogravimetry (TG) measurement was carried out from room temperature to 1200 K in a mixed Ar (96%) and H_2 (4%) gas flow with a heating rate of 10 K min^{-1} by using a Rigaku TG-8120 system. The temperature and field dependence of the magnetization was measured by using a SQUID (superconducting quantum interference device) magnetometer (Quantum Design MPMS (magnetic property measurement system)) in zero-field-cooling (ZFC) and/or field-cooling (FC) runs. The resistivity and AMR data were collected with the use of a Quantum Design PPMS (physical property measurement system). The standard four-probe method was used for the resistivity measurements on several specimens. The AMR was measured at 6 T below T_c by rotating the sample around the field direction.

3. Results and discussion

Figure 2(a) shows the powder XRD pattern of the pulverized single crystal of brownmillerite-type $SrCoO_{2.5}$. All the diffraction peaks can be well indexed on the basis of an orthorhombic structure with lattice parameters $a = 15.735$ Å, $b = 5.572$ Å, and $c = 5.466$ Å, in good agreement with the reported neutron diffraction result [10]. (In figure 2(a), the Miller indices are not shown for all the peaks.) As seen from the XRD pattern in figure 2(b), the diffraction peaks after high oxygen pressure treatment are well indexed with a cubic $Pm\bar{3}m$ perovskite structure without any trace of impurity phase. The lattice constant obtained is $a = 3.8289$ Å. The Laue diffraction pattern shown in the inset of figure 2(b) corresponds to that of the (100) plane. The unambiguous Laue spots provide convincing evidence for the present $SrCoO_3$ sample being a good single crystal. A previous study showed that the lattice constant of oxygen-deficient $SrCoO_{3-\delta}$ perovskite is clearly reduced with decreasing δ [26]. In a nearly stoichiometric $SrCoO_3$ polycrystalline sample, the a was determined to be 3.8292 Å [27]. This value is very close to the lattice parameter obtained in this study. In order to check the oxygen content directly for our single crystal, a TG measurement was performed, and it was determined as 2.95 ± 0.02.

Figure 3(a) shows the temperature dependence of the magnetization measured at 0.5 T with the field along three

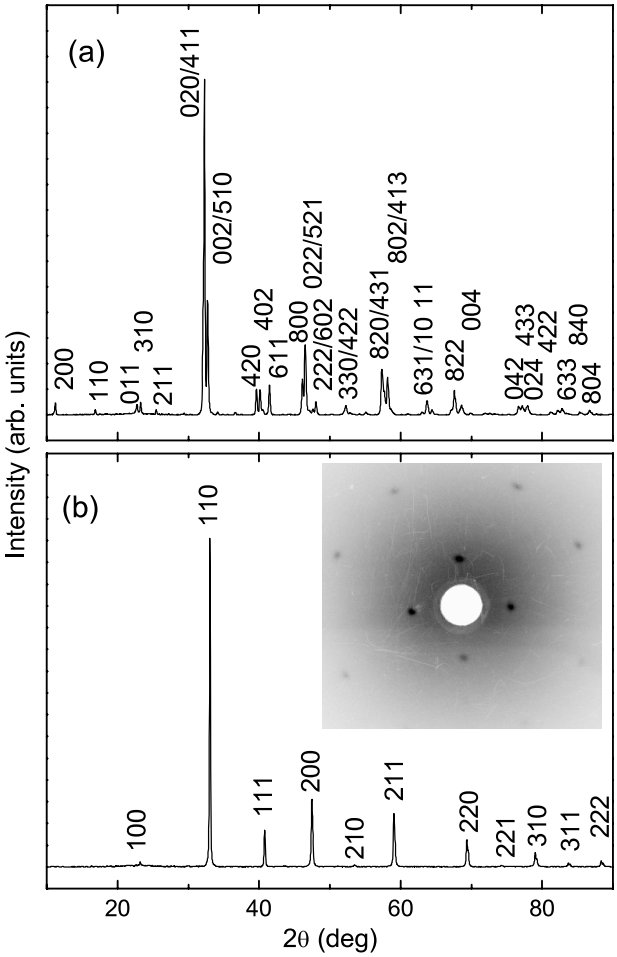

Figure 2. Powder XRD patterns and corresponding Miller indices of the pulverized single crystals of (a) brownmillerite-type $SrCoO_{2.5}$ and (b) cubic $SrCoO_3$ perovskite. The inset of (b) shows the Laue diffraction pattern with fourfold symmetry of the (100) plane of the $SrCoO_3$ single crystal.

highly symmetric crystal axes: [100], [110], and [111], and the largest magnetization is observed when the field is applied along the [111] direction. The present crystal displays a well-defined FM transition around 305 K. In the previous studies on polycrystalline samples [13, 15], the highest value of T_c is about 280 K. The present crystal has a considerably higher T_c value. The magnetization was also measured for several different pieces from the same crystal batch, and all of them exhibited identical FM Curie temperatures as well as saturation moments, indicating a homogeneous chemical composition in the present crystal.

For $SrCoO_3$ polycrystalline samples, semiconductor-like and/or poor metallic behaviors were observed due to grain boundary effects [15, 18, 28]. In contrast, our single crystal shows a good metallic behavior, as shown in figure 3(b), where the resistivity data for two different specimens A and B are presented. In accordance with the FM transition, slight anomalies are discernible in the resistivity curves. Since the chemical composition is homogeneous as described above, the difference in magnitude of resistivity between samples A and B is probably attributable to microcracks within the samples

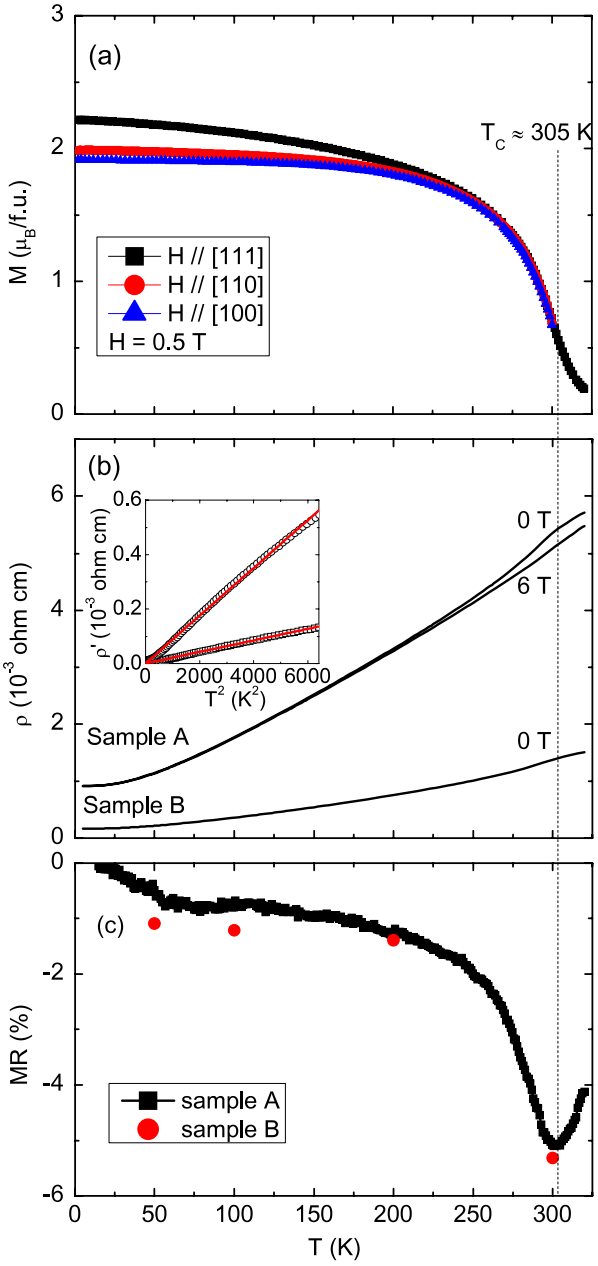

Figure 3. Temperature dependence of the magnetic and transport properties of $SrCoO_3$ single crystal. (a) Magnetization measured at 0.5 T for three field directions in FC runs. (b) Resistivity measured for a specimen with unknown orientation (sample A) at 0 and 6 T and for another specimen with current parallel to the (100) plane (sample B) at zero field. The inset shows the T^2 dependence of the resistivity below 80 K. The open circles represent experimental data, and the lines the result of fitting. (c) Magnetoresistance defined as $[\rho(6\,\mathrm{T}) - \rho(0)]/\rho(0)$ for sample A (squares) and B (dots) plotted against temperature. The data were taken by sweeping the temperature for sample A and sweeping the magnetic field at fixed temperatures for sample B.

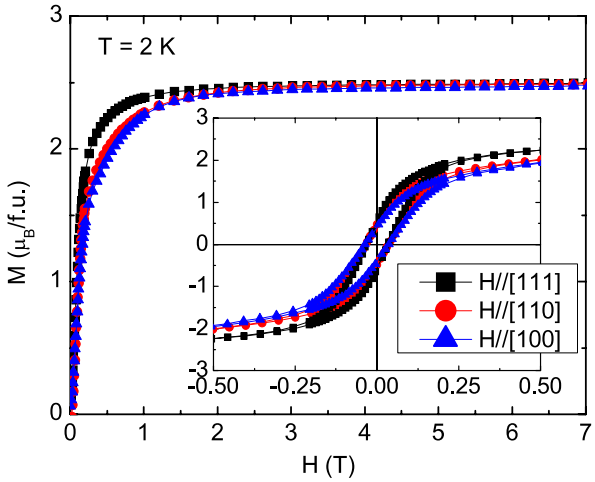

Figure 4. Field dependence of the magnetization of a $SrCoO_3$ single crystal measured at 2 K in a ZFC condition with the field along different high symmetry crystal axes. The inset shows the magnification of the low field region.

which might be caused by the high pressure treatment. In spite of this difference, both of the resistivity curves show the T^2 dependence in a wide temperature region below about 80 K, as shown in the inset of figure 3(b). Considering the FM nature, this T^2 dependence can be ascribed not to the conventional spin fluctuation effect, but, possibly, to the fluctuation in the orbital sector of the intermediate spin state.

To observe a magnetic field effect on the charge transport, the resistivity of sample A was measured also in a magnetic field of 6 T (figure 3(b)). The calculated magnetoresistance (MR) magnitude (=$[\rho(6\ \mathrm{T}) - \rho(0)]/\rho(0)$) is shown in figure 3(c). Clearly, a negative MR effect is observed over a rather wide temperature region, due to the suppression of the spin scattering. In particular, the magnitude of the MR takes a maximum value of about 5% around T_c, and decreases monotonically toward low temperatures. This behavior is characteristic of a single-crystalline sample of FM metal and is well understood in terms of the field suppression of the spin fluctuation that becomes maximal at T_c [29, 30]. Besides this, the MR effect was also studied for sample B by sweeping the field at fixed temperatures, and the values obtained at 6 T are plotted in figure 3(c). The two samples show similar MR values.

Figure 4 shows the anisotropy of the magnetization curves at 2 K with fields also along the [100], [110], and [111] directions. In the low field region, the magnetization sharply increases with increasing field, and the largest moment is observed when the field is applied parallel to [111]. This means that the easy magnetization axis is along [111] in $SrCoO_3$ single crystal, in agreement with the temperature dependent magnetization (figure 3(a)). Above 3 T, almost no difference is discernible for the three field directions. The saturation moment observed at 7 T is about 2.5 μ_B/Co^{4+}, significantly larger than the values reported previously for polycrystalline samples [15, 27]. The low spin configuration of the Co^{4+} ion ($t_{2g}^5 e_g^0$) should have a moment less than 1 μ_B/Co^{4+}, and therefore can be ruled out from this experimental observation. The intermediate spin configuration of the Co^{4+} ion ($t_{2g}^4 e_g^1$) should have a moment comparable to or slightly less than 3 μ_B/Co^{4+}, which is close to the experimental one. Therefore, the ground state of the Co^{4+} ion in $SrCoO_3$ appears to be an intermediate spin state, in accordance with the theoretical

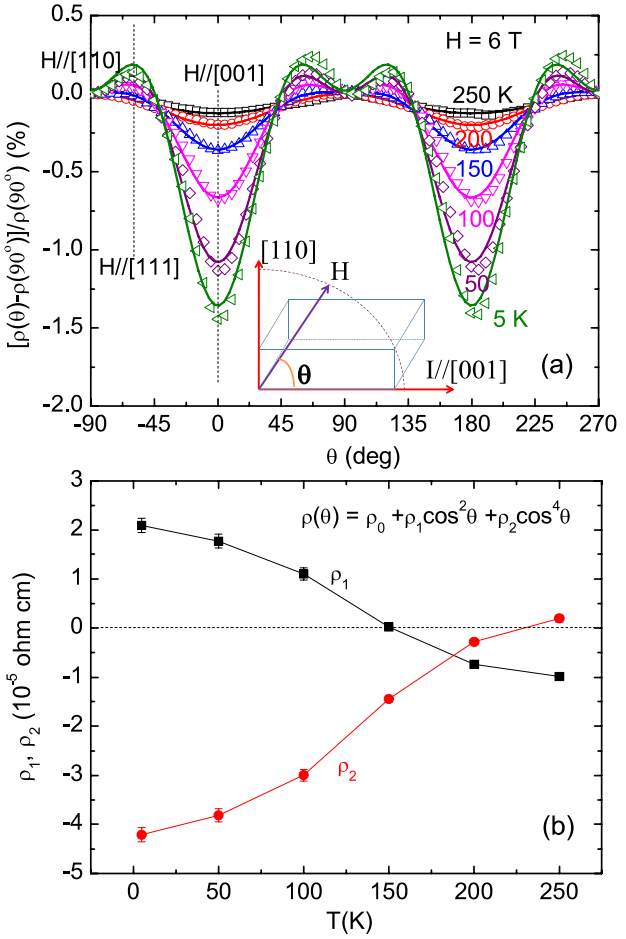

Figure 5. (a) Field-orientation dependence of the normalized AMR of the $SrCoO_3$ single crystal. The symbols show the experimental data and the curves represent the results of a fitting using the function $\rho(\theta) = \rho_0 + \rho_1 \cos^2\theta + \rho_2 \cos^4\theta$, where θ denotes the angle between the current and magnetic field directions. The inset shows the geometrical configuration for the AMR measurement. (b) The fitted parameters, ρ_1 and ρ_2, as a function of temperature.

prediction [14]. As shown in the inset of figure 4, the coercive force in the present cubic $SrCoO_3$ sample is only about 0.03 T for all the directions and the hysteresis is quite small. This is very different from the case for the tetragonal (K_2NiF_4-type structure) Sr_2CoO_4 thin film sample, where a coercive force as large as 2.2 T was found for the easy-axis (c-axis) magnetization process [31].

To investigate possible effects of the magnetic field direction on the transport properties, we measured the AMR. The inset of figure 5(a) shows the geometrical configuration of the AMR measurement on the $SrCoO_3$ crystal. Here a (110) plate of the crystal was used for the AMR study. The current direction was along the [001] axis, while a field of 6 T was rotated around the [1$\bar{1}$0] axis. We defined the rotation angle as $\theta = 0$ deg when $H \parallel [001]$, i.e., with the field parallel to the current, following the convention of [32]. In this definition, the field direction coincides with the [111] axis at $\theta = 55°$ and the [110] axis at $\theta = 90°$.

Figure 5(a) shows the normalized AMR ($=[\rho(\theta) - \rho(90°)]/\rho(90°)$) of $SrCoO_3$ measured at different temperatures. Near T_c, the angular dependence is almost twofold symmetric with the presence of a minimum at $\theta = 0$ ($H \parallel I$) and a maximum at $\theta = 90°$ ($H \perp I$). With decreasing temperature, however, a striking change occurs in the angle dependence; the maximum of AMR appears around $\theta = 55°$, i.e., the $H \parallel [111]$ direction. Further lowering the temperature enhances this tendency. As shown in figure 5(a), the data are nicely fitted using the formula $\rho(\theta) = \rho_0 + \rho_1 \cos^2\theta + \rho_2 \cos^4\theta$. The fitting parameters ρ_1 and ρ_2 are plotted against temperature in figure 5(b). Above 200 K, the value of ρ_2 is rather small, suggesting that the contribution of the $\cos^4\theta$ term is not so significant. However, with decreasing temperature, ρ_2 increases in magnitude with negative sign. Also, ρ_1 changes sign around 150 K.

For many FM metallic systems, including conventional FM metals and perovskite-type manganites, when the magnetization is saturated by the magnetic field, the AMR is often well expressed with the $\cos^2\theta$ term alone [32–35]. In the present measurement, the applied field (6 T) is much larger than the saturation field, as shown in figure 4. Therefore, the magnetization is isotropic at this high field. Even in this case, however, the AMR with a $\cos^4\theta$ term is observed at low temperatures, while the $\cos^2\theta$ term is dominant above 200 K. This $\cos^2\theta$ term at high temperatures should be ascribed to the classical effect of the Lorenz force, i.e., transverse versus longitudinal MR, but for the unusual AMR with the $\cos^4\theta$ term observed at low temperatures, we should take into account the electronic configuration of Co^{4+} in detail.

As we inferred from the magnetization, an intermediate spin state ($3d^5$: $t_{2g}^4 e_g^1$) of Co^{4+} would be the most probable configuration. According to the theoretical calculation [22], the four t_{2g} electrons form narrow bands, and hence their orbitals and spins would be considered to be well polarized even in the metallic state. The number of t_{2g} electrons is the one major difference between the present material and manganites (three t_{2g} electrons). In the case of manganites, the AMR described by the $\cos^2\theta$ term is observed and explained in terms of the field direction dependent modification of e_g bands originating from the spin–orbit interaction, even with the assumption of an isotropic scattering rate. In addition to the e_g sector (conduction electrons), one extra electron with minority spin in the t_{2g} sector should be taken into account in the present case, and the presence of this t_{2g} down spin would give rise to crystalline anisotropy as well as the anisotropic scattering rate [36, 37], which depends on the magnetization direction and the wavevector of the conduction electron, although an elaborate theory would be necessary for quantitatively elucidating the dominant contribution of the $\cos^4\theta$ term.

4. Conclusions

In summary, we succeeded in synthesizing the cubic perovskite $SrCoO_3$ single crystal with nearly stoichiometric oxygen content. Considering the similarity in structure between the orthorhombic brownmillerite-type $SrCoO_{2.5}$ and the cubic perovskite-type $SrCoO_3$, a $SrCoO_{2.5}$ single crystal was first prepared as a precursor by a floating-zone method. Then, this

oxygen-deficient crystal was treated by high oxygen pressure annealing at 6.5 GPa and 1023 K. This combined technique proved to be very effective for obtaining $SrCoO_3$ single crystal with nearly stoichiometric oxygen content (2.95 ± 0.02). This method would also allow preparing other perovskite single crystals with unusually high valence transition metal ions.

FM ordering was found to occur in the present synthesized $SrCoO_3$ crystal at around 305 K; this Curie temperature is higher than all other values reported for polycrystalline samples, by more than 20 K. The [111] crystal axis was found to be the easy magnetization axis. The observed saturation moment at 2 K (2.5 μ_B/f.u.) indicated that an intermediate spin Co^{4+} state is most probable in $SrCoO_3$, although the real ground state should be regarded as strongly hybridizing with the $3d^6\underline{L}$ state, namely, a high spin Co^{3+} state ($3d^6$: $t_{2g}^4e_g^2$) with an oxygen hole $\underline{L}$ [14]. Considering the minimal spin fluctuation in the FM metallic ground state, the observed T^2 dependence of the resistivity at low temperatures may indicate scattering of conduction electrons by orbital fluctuation inherent to such an intermediate spin state. While $SrCoO_3$ possesses a highly symmetric cubic structure, AMR with a significant $\cos^4\theta$ term was found for the saturated magnetization state, where the magnetization shows no anisotropy. The anisotropic rate of scattering of conduction electrons by the localized t_{2g} spin (t_{2g}^4) was assigned as the origin of the unusual AMR effect.

Acknowledgments

The authors thank Y Tokunaga, A Kikkawa, and H Sakai for help with the AMR and TG experiments. This work was partly supported by the Funding Program for World-Leading Innovative R&D on Science and Technology (FIRST Program) on 'Quantum Science on Strong Correlation' of JSPS.

References

[1] Shao Z P and Haile S M 2004 *Nature* **431** 170
[2] Vashook V V, Zinkevich M V and Zonov Y G 1999 *Solid State Ion.* **116** 129
[3] Korotin M A, Ezhov S Y, Solovyev I V, Anisimov V I, Khomskii D I and Sawatzky G A 1996 *Phys. Rev.* B **54** 5309
[4] Saitoh T, Mizokawa T, Fujimori A, Abbate M, Takeda Y and Takano M 1997 *Phys. Rev.* B **55** 4257
[5] Zobel C, Kriener M, Bruns D, Baier J, Grüninger M, Lorenz T, Reutler P and Revcolevschi A 2002 *Phys. Rev.* B **66** 020402
[6] Haverkort M W *et al* 2006 *Phys. Rev. Lett.* **97** 176405
[7] Belik A A *et al* 2006 *Chem. Mater.* **18** 798
[8] Oka K *et al* 2010 *J. Am. Chem. Soc.* **132** 9438
[9] Toquin R L, Paulus W, Cousson A, Prestipino C and Lamberti C 2006 *J. Am. Chem. Soc.* **128** 13161
[10] Muñoz A, de la Calle C, Alonso J A, Botta P M, Pardo V, Baldomir D and Rivas J 2008 *Phys. Rev.* B **78** 054404
[11] Takeda Y, Kanno R, Takada T, Yamamoto O, Takano M and Bando Y 1986 *Z. Anorg. Allg. Chem.* **540** 259
[12] Nemudry A, Rudolf P and Schöllhorn R 1996 *Chem. Mater.* **8** 2232
[13] Kawasaki S, Takano M and Takeda Y 1996 *J. Solid State Chem.* **121** 174
[14] Potze R H, Sawatzky G A and Abbate M 1995 *Phys. Rev.* B **51** 11501
[15] Bezdicka P, Wattiaux A, Grenier J C, Pouchard M and Hagenmuller P 1993 *Z. Anorg. Allg. Chem.* **619** 7
[16] Balamurugan S, Yamaura K, Karki A B, Young D P, Arai M and Takayama-Muromachi E 2006 *Phys. Rev.* B **74** 172406
[17] Taguchi H, Shimada M, Kanamaru F, Koizumi M and Takeda Y 1976 *J. Solid State Chem.* **18** 299
[18] Takeda T and Watanabe H 1972 *J. Phys. Soc. Japan* **33** 973
[19] Battle P D, Green M A, Lago J, Mihut A, Rosseinsky M J, Spring L E, Singleton J and Vente J F 1998 *Chem. Commun.* **9** 987
[20] Bahadur D, Kollali S, Rao C N R, Patni M J and Srivastava C M 1979 *J. Phys. Chem. Solids* **40** 981
[21] Taguchi H, Shimada M and Koizumi M 1980 *Mater. Res. Bull.* **15** 165
[22] Zhuang M, Zhang W, Hu A and Ming N 1998 *Phys. Rev.* B **57** 13655
[23] Takei H, Oda H, Watanabe H and Shindo I 1978 *J. Mater. Sci.* **13** 519
[24] Nakatsuka A, Yoshiasa A, Nakayama N, Mizota T and Takei H 2004 *Acta Crystallogr.* C **60** i59
[25] Grenier J G, Ghodbane S, Demazeau G, Pouchard M and Hagenmuller P 1979 *Mater. Res. Bull.* **14** 831
[26] Taguchi H, Shimada M and Koizumi M 1979 *J. Solid State Chem.* **29** 221
[27] Balamurugan S and Takayama-Muromachi E 2006 *J. Solid State Chem.* **179** 2231
[28] Ido T, Yasui Y and Sato M 2003 *J. Phys. Soc. Japan* **72** 357
[29] Hwang H Y, Cheong S-W, Ong N P and Batlogg B 1996 *Phys. Rev. Lett.* **77** 2041
[30] Taguchi Y and Tokura Y 1999 *Phys. Rev.* B **60** 10280
[31] Matsuno J, Okimoto Y, Fang Z, Yu X Z, Matsui Y, Nagaosa N, Kawasaki M and Tokura Y 2004 *Phys. Rev. Lett.* **93** 167202
[32] Fuhr J D, Granada M, Steren L B and Alascio B 2010 *J. Phys.: Condens. Matter* **22** 146001
[33] Khmelevskyi S, Palotás K, Szunyogh L and Weinberger P 2003 *Phys. Rev.* B **68** 012402
[34] Bibes M, Martínez B, Fontcuberta J, Trtik V, Ferrater C, Sánchez F, Varela M, Hiergeist R and Steenbeck K 2000 *J. Magn. Magn. Mater.* **211** 206
[35] Li R, Wang H, Wang X, Yu X Z, Matsui Y, Cheng Z, Shen B, Plummer E W and Zhang J 2009 *Proc. Natl Acad. Sci. USA* **106** 14224
[36] Smit J 1951 *Physica* **17** 612
[37] Campbell I A, Fert A and Jaoul O 1970 *J. Phys. C: Solid State Phys.* **3** S95